

Electronic Structures of Niobium Carbides: NbC_n (n = 3–8)

Dingguo Dai,[†] S. Roszak,^{†,‡} and K. Balasubramanian^{*,†}

Department of Chemistry and Biochemistry, Arizona State University, Tempe, Arizona 85287-1604, USA, and Institute of Physical and Theoretical Chemistry, Wrocław University of Technology, Wyb. Wyspińskiego 27, 50–370 Wrocław, Poland

Received: April 14, 2000; In Final Form: August 14, 2000

The low-lying electronic states of NbC_n with five different geometries, namely, ring (R), linear (L), kite (K), Nb-terminally bound to a C_n ring (T), and a structure with C–Nb–C bridge fused with a C_n ring (A) (n > 3) are considered for n = 3–8. Three different levels of theoretical techniques, viz., complete active space multiconfiguration self-consistent field, multireference singles + doubles configuration interaction, and density functional theory were considered. We compute the equilibrium geometries, energy separations of the low-lying electronic states, Gibbs free energies, and heat capacity functions as a function of temperatures. For smaller clusters such as NbC₃, NbC₄, and NbC₅, we find the ring structure to be lower with the linear structure as the first excited structure. Larger clusters exhibit odd–even alternation in that for even n the linear and ring structures are very close, whereas the clusters with odd n exhibit lower ring structures analogous to the smaller clusters. NbC₆ was found to be unusual in having a linear ground state.

I. Introduction

Transition metal carbides have a long and rich history of experimental and theoretical studies.^{1–46} A possible motivation for these studies is that the transition metal catalysts find extensive use in reforming petroleum-based products. Thus, there is a compelling need to comprehend the nature of metal–carbon bonds, as this could aid in the understanding of catalytic selectivity and mechanisms. Although earlier experimental studies were carried out using the Knudsen effusion technique combined with mass spectrometry,^{4–7} more recent studies have included the ion drift tube technique,^{2,9–11} electron spin resonance spectroscopy^{14–17} of rare-gas matrix isolated carbides, and high-resolution optical spectroscopy.^{12,13,18–22} Larger transition metal carbide clusters such as LaC_n⁺² and TaC_n^{+3,40} have also been studied for many values of n. High-resolution optical spectroscopic techniques have been employed on diatomic carbides containing second row transition metal atoms such as YC,¹³ NbC,¹² and PdC.¹⁹ Photoelectron spectroscopy of the anion has also yielded information on the neutral WC.¹⁸ The matrix-isolated ESR spectroscopy has been utilized on second-row transition metal carbides.^{14–17}

There is also significant interest on larger transition metal carbon clusters such as metallofullerenes,¹ metallocarbohedranes, and unusually stable “metcars”,³⁹ as these species exhibit unusual stability and bonding characteristics with potential industrial applications. A recent review article of Rohmer et al.⁵ summarizes advances pertinent to not only larger transition metal carbides such as metcars but also smaller transition metal carbides.

There have been several experimental studies on niobium carbides and their ions. The mass spectroscopic studies made by Duncan and co-workers⁴² as well as Castleman and co-workers⁴¹ have revealed that among the smaller Nb_nC_n⁺ clusters,

especially for n = 2–4, are particularly stable. The binding energies with –OH and –OCH₃ groups have been estimated for the niobium carbide clusters with abstraction reactions between H₂O and Nb₄C₄⁺. Larger Niobium carbide clusters with two types of compositions have been found to be especially very abundant, and they correspond to metcars and fcc crystallites.

Spectroscopic studies on smaller niobium carbides include the matrix-isolated ESR spectroscopy of NbC by Hamrick and Weltner,¹⁴ which have yielded the spin multiplicity of the ground state of the diatomic NbC. Simard and co-workers¹² have obtained the spectroscopic constants of several low-lying electronic states of the diatomic NbC through optical spectroscopy.

Theoretical studies have been focused primarily on the second-row transition metal carbides such as YC,⁸ MoC,³⁵ RuC,³⁴ RhC²⁹, and PdC.^{32,33,36–38} The earlier studies have been typically made using the Hartree–Fock/Configuration interaction (HF/CI) techniques.^{8,32–35} The RhC²⁹ and PdC³⁸ diatomics have been studied using complete active space multiconfiguration self-consistent field (CAS-MCSCF) followed by multireference singles + doubles configuration interaction (MRSDCI) techniques. There have been a few studies from our laboratory^{23–26} on transition metal carbides containing multiple number of carbon atoms such as YC_n, TaC_n, LaC_n, etc. There have also been RHF and MP2 studies on Nb₄C₄ cluster and its cation.⁴³ Among other transition metal carbides, there have extensive number of studies on iron carbides.^{44–46}

The relative energy ordering of the electronic states is often uncertain, as different levels of theory do not always yield the same information. This is a consequence of a large number of low-lying electronic states of different spin multiplicities and spatial symmetries for transition metal carbides. There is a competition between spin exchange stabilization and electron correlation. The spin exchange stabilization favors the high spin electronic states, whereas electron correlation effects stabilize the low-spin electronic states, and thus, the competition between

* To whom correspondence should be addressed. E-mail: kbalu@asu.edu.

[†] Department of Chemistry and Biochemistry, Arizona State University.

[‡] Institute of Physical and Theoretical Chemistry, Wrocław University of Technology.

the two stabilization features places the electronic states at different relative energies at different levels of theory. In addition, relativistic effects⁴⁷ make significant contributions to the second and third row transition metal carbides.

Although the diatomic NbC has been studied experimentally before, this is not the case with larger NbC_n clusters. At present, very little information is available on larger clusters. The above survey reveals significant current interest in transition metal carbides. These species exhibit a large number of low-lying quartet and doublet electronic states and the nature of bonding in these states seem to differ due to differences in the participation of Nb(4d), Nb(5s), and Nb(5p) orbitals. We also calibrate the utility of the density functional theory (DFT) and the CASMCSCF/MRSDCI techniques for these carbides. The objectives of the current study are computations of the equilibrium geometries and energy separations of the NbC_n clusters. We have also computed the thermodynamic properties (enthalpies and Gibbs free energies) of these species. We have investigated several low-lying high spin and low spin electronic states at the CASMCSCF and MRSDCI levels that included multi-million configurations. We have also carried out computations at the DFT level for the low-lying electronic states to facilitate comparison of the DFT and CASMCSCF/MRSDCI techniques.

II. Method of Calculation

The niobium carbide clusters have been studied at different levels of theory here. Although for all clusters, a variety of structures were considered at the density functional level of theory (DFT), for the NbC_n ($n = 3-6$) clusters, the CASMCSCF technique was followed by the MRSDCI scheme was utilized. The CASMCSCF/MRSDCI techniques were used to gauge the accuracy of the DFT technique. The DFT technique was employed in conjunction with Becke's⁵⁵ three-parameter hybrid method using the LYP correlation functional (B3LYP). Geometries of different low-lying electronic states often with different spin multiplicities were optimized at the B3LYP, CASMCSCF, and MRSDCI levels, whereas the vibrational frequencies were calculated at the B3LYP level.

All of the computations were carried out using relativistic effective core potentials (RECPs) for the Nb atom taken from La John et al.,⁴⁸ which retained the outer 4s²4p⁶4d⁴5s¹ shells of the niobium atom in the valence space, replacing the remaining core electrons by RECPs. The RECPs for the carbon atom retained the outer 2s²2p² shells in the valence space. The optimized valence (5s5p4d) Gaussian basis sets for the Nb atom were taken from ref 48. The (4s4p) optimized Gaussian basis sets for the carbon atoms were contracted to (3s3p). The carbon basis set was supplemented with a set of six-component 3d functions with $\alpha_d = 0.75$. Our final basis sets are (5s5p4d) for the Nb atom and (3s3p1d) for the carbon atoms. The effect of 4f functions was studied,³¹ and it was found that the inclusion of 4f functions change the M-C bond lengths by 0.01 Å and relative energy separations by 0.01–0.1 eV. Consequently, we do not anticipate the 4f type of functions to make significant contributions.

Different types of structures, such as the ring, kite, linear, ring with tail, and fused bicyclic structures, were considered. Full geometry optimization was considered for each of these structures for different electronic states. Using these data, the thermodynamic properties such as the Gibbs free energies and heat content functions were computed. The vibrational frequencies and IR intensities were also computed for the minimal

energy structures, and the existence of all real frequencies confirm that the minimal geometries report here were true minima.

The CASMCSCF computations of the clusters followed by MRSDCI computations were carried out for the smaller NbC_n clusters with $n = 3-6$ in order to gauge the accuracy of the DFT computations. On the basis of the accuracy, the DFT technique was employed for all of the clusters considered here. Separate CASMCSCF calculations for the electronic states of different spatial symmetries and spin multiplicities were carried out. These computations were carried out in the C_{2v} group as all of the structures considered here have at least C_{2v} symmetry. The 4s and 4p orbitals of the Nb atom that correlate into two a₁, one b₂, one b₁ orbitals were kept inactive in that no excitations from these shells were allowed but they were allowed to relax. Among the remaining orbitals, up to 9 orbitals were included in the active space (8–10 inactive orbitals) so as to represent all of the electronic states of NbC_n adequately. Up to 11 active electrons were distributed in all possible ways among the active orbitals in CASMCSCF. The remaining electrons were kept inactive. Let a quadruple of numbers represent the number of orbitals in a₁, b₂, b₁, and a₂ irreducible representations of the C_{2v} group. For NbC₃, the of inactive orbitals are given by N_i = 3 2 2 0 and the number of active orbitals are given by N_a = 4 2 2 1. The corresponding quadruples for NbC₄ are N_i = 5 2 2 0 and N_a = 4 2 2 1. For NbC₅ these numbers are given by N_i = 5 3 2 1 and N_a = 4 2 2 1. In summary, the CASMCSCF computations were carried out with sufficient flexibility yet keeping the orbital space manageable so that the number of configuration spin functions (CSFs) is not too big.

Following CASMCSCF, MRSDCI calculations were carried out for all of the low-lying quartet, doublet and sextet electronic states of NbC_n to include the effects of higher-order electron correlation effects. The reference configurations for the MRSDCI computations were chosen from the CASMCSCF calculations with absolute coefficients ≥ 0.07 . All possible single and double excitations were allowed at the MRSDCI. The MRSDCI computations included a multi-million-configuration space. The DFT/B3LYP⁵⁵ computations were made with the Gaussian 98 codes.⁵⁶

The spin-orbit effects were estimated for NbC₂ on the basis of the Nb atomic spin-orbit splittings⁵⁷ and the contribution of the Nb orbitals to the open-shell orbitals of NbC₂. The spin-orbit effects were found to be rather small if the carbon orbitals make substantial contribution to the open-shell orbitals since the spin-orbit effects on the carbons⁵⁷ are less than 100 cm⁻¹.

All CASMCSCF/MRSDCI calculations were made using a modified version⁵² of ALCHEMY II codes⁵¹ to include the RECPs.

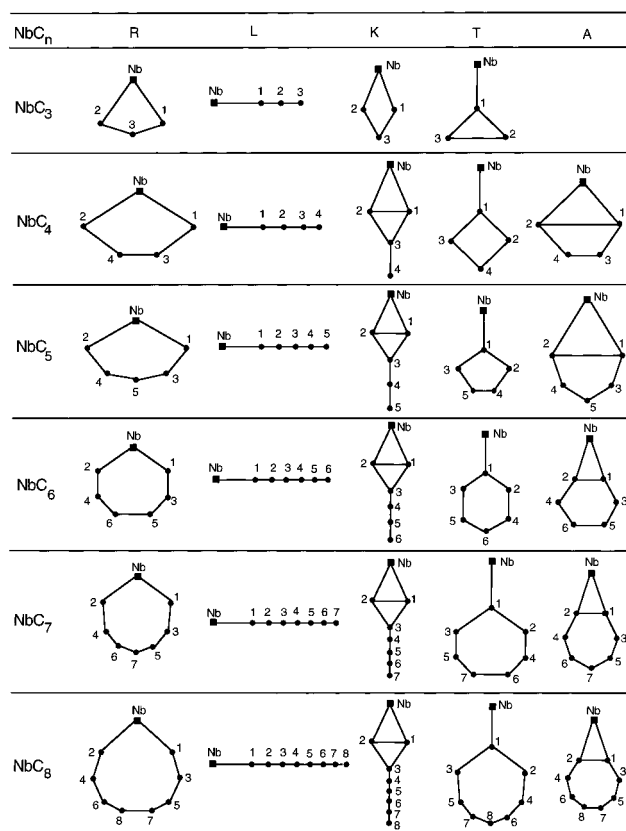
III. Results and Discussion

The electronic states of niobium carbides could arise from the Nb(4F) ground state or the low-lying Nb doublet electronic state⁵⁷ and one of the low-lying singlet or triplet states of the naked C_n cluster. This would result in quartet, doublet and sextet electronic states for NbC_n. We expect the sextet states to be higher in energy on the basis of our previous electronic structure studies on NbC₂.³¹ We have thus considered exhaustive study of the doublet, quartet, and sextet electronic states for these species. We have considered four kinds of structures for all of the electronic states. These structures are (1) a ring structure (R) in which the Nb atom is inserted in to the C_n ring and it is part of the ring as in Figure 1, (2) the Nb atom is at the terminal of a linear structure (L) (3) a tail of carbon atoms attached to a

TABLE 1: Geometries and Energy Separations of the Electronic States of NbC₃ at B3LYP Level

structure	state	geometry ^a						E(B3LYP) (eV)
		Nb-C ₁	C ₁ -C ₂	C ₁ -C ₃	C ₂ -C ₃	a ₁	a ₂	
R	² A ₁	1.957	2.483	1.344	1.344	78.7	134.9	0.00
	⁴ B ₂	2.099	2.494	1.324	1.324	72.9	140.8	0.98
	⁶ A ₁	2.199	2.497	1.328	1.328	69.2	140.2	1.79
L	⁶ Σ	1.989	1.294		1.301	180	180	1.49
	doublet	1.880	1.319		1.287	180	180	1.86
	quartet	1.973	1.293		1.302	180	180	2.03
K	⁴ B ₁	2.091	1.431	1.416	1.416	40.0	60.7	1.79
	⁶ B ₂	2.173	1.530	1.355	1.355	41.2	68.8	2.11
	² A ₁	2.051	1.408	1.411	1.411	40.2	59.9	2.63
T	⁴ B ₁	2.015	1.440	1.440	1.348	152.1	55.8	2.42
	⁶ A ₁	2.091	1.430	1.430	1.328	152.3	55.3	2.73
	² A ₁	2.061	1.423	1.423	1.364	151.4	57.3	3.56

^a For the R structure, a₁ represents the bond angle of C₁-Nb-C₂, a₂ represents the bond angle of C₁-C₃-C₂. For the K structure, a₁ represents the bond angle of C₁-Nb-C₂, a₂ represents the bond angle of C₁-C₃-C₂. For the T structure, a₁ represents the bond angle of Nb-C₁-C₂ and Nb-C₁-C₃, a₂ represents the bond angle of C₂-C₁-C₃.

**Figure 1.** Geometries of NbC_n considered here.

four-member ring containing the Nb atom which we call the kite structure (K) as in Figure 1, (3) Nb bound terminally as a pending bond to a cyclic C_n structure (T; Figure 1), and (4) a bicyclic fused system containing a C-Nb-C triangular ring. As we shall see from our results, some of these structures are viable candidates for the low-lying electronic structures of these clusters.

Although there appears to be no experimental studies on larger NbC_n clusters, there have been a few experimental studies on LaC_n and YC_n clusters.^{2,5,10,11} The experimental studies of Jarrold and co-workers² particularly on the LaC_n⁺ clusters have suggested the possibility of competing linear and ring-like structures for LaC_n. Analogous to this, there is also competition between structures in which the Nb atom is inside the ring versus structures in which Nb is exteriorly attached to the carbon ring. Because the species that we consider here have relatively small number of carbon atoms, stable rings could be formed with Nb

TABLE 2: Energy Separations of the Electronic States of NbC₃ at the CASSCF and MRSDCI Levels

structure	state	E (CASSCF) (eV)			E(MRSDCI) (eV)
		adiabatic	vertical (a)	vertical (b)	
R	² A ₁	0.00	0.00		0.00 (0.00)
	⁴ B ₂	0.94	1.27	0.94	1.37 (1.33)
	⁴ A ₂		1.62	0.98	
	² B ₂		1.58		
	² A ₂		1.61		
	⁴ A ₁		2.50	1.96	
	⁴ B ₁		2.96	2.45	
	² B ₁		3.26		

^a Vertical(a) at the equilibrium geometry of the ²A₁ state of the ring structure from B3LYP. ^b Vertical(b) at the equilibrium geometry of the ⁴B₂ state of the ring structure from B3LYP.

included inside the ring, rather than pure carbon rings with metal atoms attached to it. More complex structures, such as the kite structure (K in Figure 1) for medium-sized clusters are also feasible. The geometries of all of these structures were optimized at the DFT/B3LYP level of theory. Note that although we allowed for full geometry optimizations, the minimal energy structures were found to be planar for all of the smaller clusters considered here. This is not surprising in that all smaller C_n clusters are indeed planar as the planar structures support multiple bonding for smaller carbon clusters. Of course for larger carbon clusters fullerene cages are feasible, but such closed structures are not attainable for fewer than 20 carbon atoms.

NbC₃. The optimized structures for the three spin states are presented in Table 1 for NbC₃ for all four geometries that we have considered. As seen from Table 1, the ²A₁ state with a ring structure (Figure 1) of C_{2v} symmetry is the lowest in energy. The ⁴B₂ state with the same structure is 0.98 eV higher in energy, indicating a preference for a low spin ground state, even though the ground state of Nb is a ⁴F state. The sextet state with a ring structure is not a viable candidate, although the linear structure exhibits a lower ⁶Σ state. It is also interesting that only the ring structure exhibits doublet state as the lowest, whereas other structures exhibit quartet or sextet electronic states as the lowest states for those structures.

Table 2 shows the results of the CASMCSF/MRSDCI computations for several electronic states of NbC₃ with a ring structure. As seen from Table 2, the adiabatic CASMCSF energy separation of 0.94 eV for the ⁴B₂ state is very close to the DFT/B3LYP result of 0.98 eV for the same state relative to the ground state. Table 2 also reports vertical energy separations of many electronic states. Evidently, there are other very low-lying states such as ⁴A₂ close to the ⁴B₂ state.

TABLE 3: Geometries and Energy Separations of the Electronic States of NbC₄ at B3LYP Level

structure	state	geometry ^a									E(B3LYP) (eV)	
		Nb–C ₁	Nb–C ₃	C ₁ –C ₂	C ₁ –C ₃	C ₂ –C ₃	C ₂ –C ₄	C ₃ –C ₄	a ₁	a ₂		a ₃
R	⁴ B ₁	2.170	2.155	3.483	1.300		1.300	1.360	106.8	71.9	144.7	0.00
	² A ₁	2.109	2.033	3.553	1.339		1.339	1.371	114.8	68.0	144.6	0.07
	⁶ A ₁	2.360	2.362	3.519	1.290		1.290	1.340	96.4	74.2	147.6	2.66
L	quartet	1.927		1.283		1.305		1.281	180	180	180	1.07
	sextet	2.112		1.257		1.325		1.289	180	180	180	1.94
	doublet	2.118		1.258		1.318		1.289	180	180	180	3.79
K	⁴ B ₁	1.973		1.452	1.484	1.484		1.308	43.2	60.7	150.7	2.64
	² A ₁	1.923		1.520	1.458	1.458		1.314	46.6	58.6	148.6	2.90
	⁶ A ₁	2.070		1.481	1.427	1.427		1.381	41.9	58.7	148.7	3.55
A	⁶ B ₁	2.021		2.556	1.338		1.338	1.438	78.5	116.1	114.7	2.76
	⁴ B ₂	1.934		1.830	1.394		1.394	1.388	56.5	142.7	99.1	3.40
	² A ₁	1.892		1.835	1.471		1.471	1.257	58.0	139.7	101.3	3.98
T	⁴ B ₁	1.989		1.455	1.455	1.493	1.431	1.431	149.1	61.7	62.8	2.85
	⁶ A ₁	2.136		1.436	1.436	1.504	1.445	1.445	148.4	63.2	62.7	3.36
	² B ₁	1.949		1.521	1.521	2.005	1.401	1.401	138.8	82.5	91.4	6.11

^a For the R structure, a₁ represents the bond angle of C₁–Nb–C₂, a₂ represents the bond angle of Nb–C₁–C₃ and Nb–C₂–C₄, a₃ represents the bond angle of C₁–C₃–C₄ and C₂–C₄–C₃. For the K structure, a₁ represents the bond angle of C₁–Nb–C₂, a₂ represents the bond angle of C₁–C₂–C₃ and C₂–C₁–C₃, a₃ represents the bond angle of C₁–C₃–C₄ and C₂–C₃–C₄. For the A structure, a₁ represents the bond angle of C₁–Nb–C₂, a₂ represents the bond angle of Nb–C₁–C₃ and Nb–C₂–C₄, a₃ represents the bond angle of C₁–C₃–C₄ and C₂–C₄–C₃. For the T structure, a₁ represents the bond angle of Nb–C₁–C₂ and Nb–C₁–C₃, a₂ represents the bond angle of C₂–C₁–C₃, a₃ represents the bond angle of C₂–C₄–C₃.

TABLE 4: Energy Separations of the Electronic States of NbC₄ at the CASSCF and MRSDCI Levels

structure	state	E (CASSCF) (eV)			E(MRSDCI) (eV)
		adiabatic	vertical (a)	vertical (b)	
R	⁴ B ₁	0.00	0.00		0.00 (0.00)
	² A ₁	–0.04	0.004	–0.04	0.12 (0.11)
	⁴ A ₂		0.12		
	² B ₁		0.44	0.85	
	⁴ B ₂		0.85		
	² A ₂		1.00	1.77	
	² B ₂		1.86	3.26	
	⁴ A ₁		2.91		

^a Vertical(a) at the equilibrium geometry of the ⁴B₁ state of the ring structure from B3LYP. ^b Vertical(b) at the equilibrium geometry of the ²A₁ state of the ring structure from B3LYP.

In previous studies on LaC_n^{23,25} we have compared the results of the DFT calculations with those of MP2 and found that the DFT results are very similar to the MP2 results. However, NbC₃ differs from LaC₃ in that another structure called the fan structure is lower in energy compared to the kite structure. The linear structure was assumed to be the ground state for LaC₃ in thermodynamic experiments.^{3–5} The kite isomer comes out to be the ground state of YC₃. Consequently, NbC₃ differs significantly from other early transition metal carbides such as LaC₃ and YC₃.

NbC₄. Tables 3 and 4 consist of our computed results on NbC₄ at different levels of theory. As seen from Table 3, the ground state for the NbC₄ cluster is a ²B₁ (C_{2v}) electronic state with a ring structure shown in Figure 1. However, the ²A₁ state with the same structure is only 0.07 eV above this state, suggesting near-degeneracy of the two states. Analogous to NbC₃, the linear structure of NbC₄ with a quartet state is 1.07 eV higher than the ring structure. Other structures, such as the kite structure, the T-structure, and the A-structure in Figure 1, are considerably higher in energy for NbC₄. Unlike NbC₃, the kite and the T structures are considerably higher in energy for NbC₄.

As seen from Table 4, the CASSCF and MRSDCI techniques also predict the ⁴B₁ and ²A₁ states to be nearly degenerate consistent with the DFT prediction. In fact, at the CASSCF level, the ²A₁ electronic state is slightly lower in energy compared to the ⁴B₁ state. The MRSDCI+Q result is

quite close to the MRSDCI result, thus providing confidence in the MRSDCI technique and the completeness of the reference space.

Hay and co-workers⁴³ have employed RHF and MP2 computations on Nb₄C₄ and Nb₄C₄⁺ species with a *T_d* symmetry. It is interesting to note that their computed Nb–C bond distance of 2.013 Å in their structure is quite close to our Nb–C distances in NbC₄ and other niobium carbide clusters that we report here.

NbC₅. Our computed DFT results are shown in Table 5 for NbC₅. Analogous to smaller carbide clusters, NbC₅ exhibits a ring structure as the ground state with a ²A₁ state, but the linear structure becomes energetically closer to the ring structure, as seen from Table 5. The kite structure is also more stabilized relative to smaller clusters. The T-structure is particularly unfavorable. The competition of the linear structure with the ring structure is particularly interesting, as this becomes a viable candidate especially for larger clusters containing even number of carbon atoms.

The geometrical features exhibited by NbC_n clusters differ from other smaller carbide clusters such as LaC_n²³ which exhibit a preference for linear geometries although the most stable complexes of LaC_n have the fan structures.

An interesting feature that we note in Table 5 is that the Nb–C bond distances in the linear structures are usually shorter than the corresponding spin multiplets of the ring structures because Nb forms multiple bonds with carbon in the linear structure. The carbon–carbon bonds in the linear structures exhibit bond alternation analogous to the tail of the kite structures (see, Table 5).

Table 6 shows the CASSCF/MRSDCI energy separations for the ground and excited electronic states of the ring structure of NbC₅. As seen from Table 6, although at the CASSCF level the ⁴A₁–²A₁ energy separation is only 0.51 eV at the MRSDCI level this energy separation becomes 0.92 eV very close to the DFT/B3LYP result of 0.84 eV. As seen from Table 6, for NbC₅ we also find other quartet and doublet electronic states, which are potential candidates for spectroscopic observations as optical transitions to some of these states are allowed.

NbC₆. Table 7 shows the geometries and energy separations of the electronic states of NbC₆ with ring, linear, A, and the kite structures. A dramatic contrasting feature of NbC₆ is that

TABLE 5: Geometries and Energy Separations of the Electronic States of NbC₅ at B3LYP Level

structure	state	geometry ^a							E(B3LYP) (eV)	
		Nb-C ₁	C ₁ -C ₃	C ₃ -C ₅						
R		Nb-C ₁	C ₁ -C ₃	C ₃ -C ₅			a ₁	a ₂	a ₃	
	² A ₁	1.960	1.310	1.359			99.6	103.1	165.7	0.00
	⁴ A ₁	2.045	1.290	1.385			108.4	93.6	167.6	0.84
	⁶ A ₂	2.193	1.272	1.365			116.2	87.7	156.9	1.44
L		Nb-C ₁	C ₁ -C ₂	C ₂ -C ₃	C ₃ -C ₄	C ₄ -C ₅	a ₁	a ₂	a ₃	
	quartet	1.912	1.304	1.272	1.301	1.284	180	180	180	0.54
	sixtet	1.986	1.283	1.284	1.290	1.290	180	180	180	0.55
	doublet	1.865	1.319	1.264	1.306	1.284	180	180	180	0.84
K		Nb-C ₁	C ₁ -C ₂	C ₁ -C ₃	C ₃ -C ₄	C ₄ -C ₅	a ₁	a ₂	a ₃	
	⁴ B ₂	2.020	1.457	1.421	1.336	1.267	42.3	59.1	149.2	1.19
	² ?	1.989	1.480	1.426	1.337	1.267	43.7	58.7	148.7	1.59
	⁶ A ₁	2.155	1.428	1.403	1.345	1.292	38.7	59.4	149.4	2.60
A		Nb-C ₁	C ₁ -C ₂	C ₁ -C ₃	C ₃ -C ₅		a ₁	a ₂	a ₃	
	² A ₁	1.908	1.767	1.382	1.407		55.2	85.7	150.6	1.96
	⁴ A ₂	1.981	1.790	1.351	1.369		53.7	87.4	145.1	2.04
	⁶ A ₁	2.072	1.419	1.453	1.374		40.1	95.8	135.6	3.64
T		Nb-C ₁	C ₁ -C ₂	C ₂ -C ₄	C ₄ -C ₅		a ₁	a ₂	a ₃	
	² A ₁	1.980	1.453	1.409	1.370		101.9	110.7	108.4	4.93
	⁴ A ₁	1.958	1.455	1.408	1.371		102.7	110.0	108.7	5.77
	⁶ B ₂	1.963	1.456	1.410	1.375		101.9	110.7	108.3	5.87

^a For the R structure, a₁ represents the bond angle of C₁-Nb-C₂, a₂ represents the bond angle of Nb-C₁-C₃ and Nb-C₂-C₄, a₃ represents the bond angle of C₁-C₃-C₅ and C₂-C₄-C₅. For the K structure, a₁ represents the bond angle of C₁-Nb-C₂, a₂ represents the bond angle of C₁-C₂-C₃ and C₂-C₁-C₃, a₃ represents the bond angle of C₁-C₃-C₄ and C₂-C₃-C₄. For the A structure, a₁ represents the bond angle of C₁-Nb-C₂, a₂ represents the bond angle of Nb-C₁-C₃ and Nb-C₂-C₄, a₃ represents the bond angle of C₁-C₃-C₅ and C₂-C₄-C₅. For the T structure, a₁ represents the bond angle of C₂-C₁-C₃, a₂ represents the bond angle of C₁-C₂-C₄ and C₁-C₃-C₅, a₃ represents the bond angle of C₂-C₄-C₅ and C₃-C₅-C₄.

TABLE 6: Energy Separations of the Electronic States of NbC₅ at the CASSCF and MRSDCI Levels

structure	state	E (MRSDCI) (eV)		
		adiabatic	vertical	MRSDCI
R	² A ₁	0.00	0.00	0.00 (0.00)
	⁴ A ₁	0.51		0.92 (1.49)
	⁴ B ₁		1.06	
	² B ₁		1.16	
	² B ₂		2.83	
	² A ₂		2.91	
	⁴ A ₂		3.02	
	⁴ B ₂		3.47	

^a Vertical at the equilibrium geometry of the ²A₁ state of the ring structure.

it is the first Nb carbide cluster exhibiting a linear ground state, as seen from Table 7. The quartet state with a linear geometry prevails as the ground state of NbC₆ although the ring structure which is favored for the smaller niobium carbide clusters is only 0.13 eV above the linear quartet state. Note that for NbC₅ already the linear structure comes down in energy although it is still higher than the ring structure. The ring structure has two nearly-degenerate electronic states, namely, ²B₁ and ⁴B₁ states. Two electronic states with the A structure are also quite stabilized for NbC₆ although for smaller clusters, electronic states with this geometry are relatively higher in energy. On the basis of the agreement between the DFT/B3LYP technique and the CASSCF/MRSDCI techniques, all computations for larger clusters were carried out using the computationally less intensive DFT/B3LYP technique.

TABLE 7: Geometries and Energy Separations of the Electronic States of NbC₆ at B3LYP Level

structure	state	geometry ^a								E(B3LYP) (eV)
		Nb-C ₁	C ₁ -C ₂	C ₂ -C ₃	C ₃ -C ₄	C ₄ -C ₅	C ₅ -C ₆	a ₁ -a ₅		
L	quartet	1.951	1.276	1.296	1.262	1.302	1.278	180	0.00	
	doublet	1.890	1.297	1.285	1.271	1.298	1.282	180	0.46	
	sixtet	2.090	1.257	1.318	1.256	1.308	1.288	180	0.90	
R		Nb-C ₁	C ₁ -C ₃	C ₃ -C ₅	C ₅ -C ₆	a ₁	a ₂	a ₃	a ₄	
	² B ₁	1.997	1.329	1.279	1.364	94.8	125.4	158.9	118.2	0.13
	⁴ B ₁	1.994	1.326	1.283	1.340	100.2	120.4	160.2	119.3	0.15
	⁶ A ₁	2.089	1.352	1.271	1.362	115.2	105.6	164.8	122.0	1.21
A		Nb-C ₁	C ₁ -C ₃	C ₃ -C ₅	C ₅ -C ₆	a ₁	a ₂	a ₃	a ₄	
	⁴ A ₂	2.066	1.269	1.352	1.252	86.4	140.8	135.7	130.4	0.32
	² A ₁	1.959	1.305	1.296	1.297	90.1	137.7	139.0	128.2	0.49
	⁶ A ₂	2.155	1.285	1.346	1.269	85.8	143.1	128.0	136.0	2.27
K		Nb-C ₁	C ₁ -C ₂	C ₁ -C ₃	C ₃ -C ₄	C ₄ -C ₅	C ₅ -C ₆	a ₁	a ₂	
	⁴ A ₂	2.055	1.435	1.429	1.304	1.286	1.289	40.9	149.9	1.74
	² A ₁	1.924	1.553	1.445	1.305	1.287	1.289	47.6	147.5	1.90
	⁶ A ₁	2.071	1.481	1.414	1.339	1.274	1.314	41.9	148.4	2.27

^a For the R structure, a₁ represents the bond angle of C₁-Nb-C₂, a₂ represents the bond angle of Nb-C₁-C₃ and Nb-C₂-C₄, a₃ represents the bond angle of C₁-C₃-C₅ and C₂-C₄-C₆, a₄ represents the bond angle of C₃-C₅-C₆ and C₄-C₆-C₅. For the K structure, a₁ represents the bond angle of C₁-Nb-C₂, a₂ represents the bond angle of C₁-C₃-C₄ and C₂-C₃-C₄. For the A structure, a₁ represents the bond angle of C₁-Nb-C₂, a₂ represents the bond angle of Nb-C₁-C₃ and Nb-C₂-C₄, a₃ represents the bond angle of C₁-C₃-C₅ and C₂-C₄-C₆, a₄ represents the bond angle of C₃-C₅-C₆ and C₄-C₆-C₅.

TABLE 8: Geometries and Energy Separations of the Electronic States of NbC₇ at B3LYP Level

structure	state	geometry ^a								E(B3LYP) (eV)
		Nb-C ₁	C ₁ -C ₃	C ₃ -C ₅	C ₅ -C ₇	a ₁	a ₂	a ₃	a ₄	
R	² A ₁	1.954	1.299	1.318	1.297	116.9	118.2	169.7	113.8	0.00
	⁴ B ₂	2.050	1.276	1.340	1.295	117.9	115.7	169.8	114.7	0.34
	⁶ A ₁	2.195	1.273	1.350	1.288	146.0	93.1	169.5	130.5	1.45
L	quartet	1.915	1.301	1.275	1.290	1.267	1.301	1.283	180	1.18
	sextet	1.983	1.280	1.288	1.278	1.274	1.294	1.287	180	1.23
	doublet	1.858	1.322	1.261	1.301	1.261	1.306	1.283	180	1.47
A	Nb-C ₁	1.915	1.301	1.275	1.290	1.267	1.301	1.283	180	1.18
	⁴ B ₂	2.049	1.265	1.343	1.400	84.5	140.6	145.3	179.7	1.05
	² B ₂	2.009	1.279	1.325	1.390	80.2	147.0	141.8	177.8	1.59
K	Nb-C ₁	2.149	1.258	1.341	1.358	88.7	136.0	147.7	175.7	2.40
	⁴ B ₂	2.016	1.425	1.327	1.252	1.311	1.272	42.3	146.5	2.05
	² A ₁	1.928	1.437	1.324	1.255	1.306	1.276	48.7	146.5	2.39
T	Nb-C ₁	2.120	1.398	1.349	1.251	1.311	1.291	40.1	148.7	3.05
	⁶ B ₂	2.094	1.437	1.272	1.331	1.397	108.8	129.7	150.8	3.55
	⁴ A ₁	2.101	1.431	1.273	1.329	1.394	110.9	128.1	151.6	3.66
	² A ₁	2.029	1.439	1.270	1.336	1.387	113.8	125.5	152.6	4.16

^a For the R structure, a₁ represents the bond angle of C₁-Nb-C₂, a₂ represents the bond angle of Nb-C₁-C₃ and Nb-C₂-C₄, a₃ represents the bond angle of C₁-C₃-C₅ and C₂-C₄-C₆, a₄ represents the bond angle of C₃-C₅-C₇ and C₄-C₆-C₇. For the K structure, a₁ represents the bond angle of C₁-Nb-C₂, a₂ represents the bond angle of Nb-C₁-C₃ and Nb-C₂-C₄, a₃ represents the bond angle of C₁-C₃-C₅ and C₂-C₄-C₆, a₄ represents the bond angle of C₃-C₅-C₇ and C₄-C₆-C₇. For the T structure, a₁ represents the bond angle of C₂-C₁-C₃, a₂ represents the bond angle of C₁-C₂-C₄ and C₁-C₃-C₅, a₃ represents the bond angle of C₂-C₄-C₆ and C₃-C₅-C₇.

TABLE 9: Geometries and Energy Separations of the Electronic States of NbC₈ at B3LYP Level

structure	state	geometry ^a									E(B3LYP) (eV)	
		Nb-C ₁	C ₁ -C ₃	C ₃ -C ₅	C ₅ -C ₇	C ₇ -C ₈	a ₁	a ₂	a ₃	a ₄		a ₅
R	⁴ B ₁	2.073	1.267	1.325	1.261	1.317	115.0	130.1	160.6	140.2	141.5	0.00
	² B ₁	2.018	1.278	1.333	1.308	1.274	121.4	124.1	172.1	120.7	152.3	0.11
	⁶ A ₁	2.094	1.272	1.320	1.267	1.357	87.5	155.3	144.5	156.5	129.9	1.54
L	quartet	1.934	1.287	1.292	1.269	1.291	1.267	1.301	1.281	180		0.56
	sextet	2.066	1.252	1.327	1.247	1.313	1.256	1.309	1.286	180		1.09
	doublet	1.912	1.283	1.289	1.267	1.287	1.266	1.297	1.281	180		1.18
A	Nb-C ₁	1.912	1.283	1.289	1.267	1.287	1.266	1.297	1.281	180		1.18
	² A ₁	2.015	1.287	1.304	1.279	1.296	120.3	125.4	163.5	141.0	139.8	0.70
	⁴ A ₁	1.992	1.341	1.282	1.347	1.264	46.1	174.8	161.9	121.3	138.5	2.63
K	Nb-C ₁	2.082	1.294	1.336	1.301	1.305	47.1	177.4	165.1	117.7	141.0	3.24
	⁴ B ₁	1.981	1.442	1.317	1.271	1.281	1.296	1.288	43.3	149.6		2.03
	² B ₁	1.986	1.450	1.308	1.276	1.276	1.298	1.284	43.1	149.8		2.11
T	Nb-C ₁	2.072	1.408	1.343	1.256	1.296	1.285	1.299	41.7	148.4		2.41
	² B ₂	1.974	1.460	1.252	1.363	1.412	100.9	141.0	139.4	178.9	60.5	3.49
	⁶ B ₁	2.046	1.426	1.277	1.309	1.357	97.8	148.3	139.9	158.7	88.2	3.65
	⁴ B ₁	2.013	1.431	1.276	1.304	1.353	91.1	146.4	142.2	156.1	91.1	3.81

^a For the R structure, a₁ represents the bond angle of C₁-Nb-C₂, a₂ represents the bond angle of Nb-C₁-C₃ and Nb-C₂-C₄, a₃ represents the bond angle of C₁-C₃-C₅ and C₂-C₄-C₆, a₄ represents the bond angle of C₃-C₅-C₇ and C₄-C₆-C₈, a₅ represents the bond angle of C₅-C₇-C₈ and C₆-C₈-C₇. For the K structure, a₁ represents the bond angle of C₁-Nb-C₂, a₂ represents the bond angle of C₁-C₃-C₄ and C₂-C₃-C₄. For the A structure, a₁ represents the bond angle of C₁-Nb-C₂, a₂ represents the bond angle of Nb-C₁-C₃ and Nb-C₂-C₄, a₃ represents the bond angle of C₁-C₃-C₅ and C₂-C₄-C₆, a₄ represents the bond angle of C₃-C₅-C₇ and C₄-C₆-C₈, a₅ represents the bond angle of C₅-C₇-C₈ and C₆-C₈-C₇. For the T structure, a₁ represents the bond angle of C₂-C₁-C₃, a₂ represents the bond angle of C₁-C₂-C₄ and C₁-C₃-C₅, a₃ represents the bond angle of C₂-C₄-C₆ and C₃-C₅-C₇, a₄ represents the bond angle of C₄-C₆-C₈ and C₅-C₇-C₈.

The C-C bonds exhibit bond alternation for the linear and ring structures. This is consistent with the delocalization of the π -electrons in the C-C framework. The Nb-C distance is the shortest for the linear structure, as seen from Table 7.

NbC₇. Table 8 shows the computed properties and energy separations of the electronic states of NbC₇. It can be seen from Table 8 that, unlike NbC₆, the NbC₇ cluster exhibits a ring structure with a ²A₁ state as the ground state. The quartet state is only 0.34 eV higher than the doublet state for the NbC₇ cluster. The electronic states with the linear structure are

substantially higher in energy. In fact, the lowest electronic state with the linear geometry is even higher than the lowest state with the A-structure for NbC₇. This suggests a trend of odd-even alternation in that only for even n the linear structure appears to be favored, whereas for odd values of n , the ring structures are decisively more stable than the linear structures.

It may be seen from Table 8 that for the ring structure the doublet-quartet energy separation is 0.34 eV for NbC₇, whereas the two electronic states are nearly degenerate for NbC₆. The near-degeneracy of the quartet and doublet electronic states may

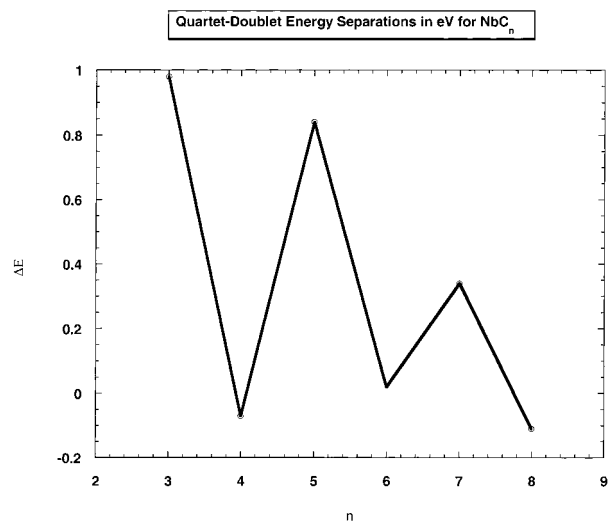


Figure 2. Plot of quartet-doublet energy separations for the ring structures of NbC_n for $n = 3-8$.

also be seen for other smaller even-numbered carbide clusters, whereas odd numbered carbide clusters exhibit a considerably larger energy splitting.

NbC_8 . Table 9 consists of the properties and energy separations of the electronic states of NbC_8 . The NbC_8 cluster exhibits a ring structure with a $^4\text{B}_1$ state as the ground state, whereas the linear states are not too far from the ring structures. The doublet state is only 0.11 eV higher than the quartet state for the NbC_8 cluster. The doublet and quartet states of the ring structure are very close in energy for the ring structure. The A-structure is also more stabilized relative to smaller clusters.

The analysis of the geometrical and electronic trends for the niobium carbide clusters clearly suggests a general trend of odd-even alternation that we briefly discussed above. That is, for even numbered clusters the energy separations between the ring and linear structures are rather small; in contrast, the odd clusters exhibit considerably larger energy separations for the linear structures. In fact, NbC_6 is very special in having a linear ground-state structure in contrast to the other carbides, which exhibit ring structures as the ground states.

We have plotted the quartet-doublet energy separations for the NbC_n clusters as a function of n for the ring structure in Figure 2. A striking feature seen from Figure 2 is odd-even alternation in that for even n clusters the quartet electronic state is close to the double state, whereas for the odd clusters the doublet electronic states are significantly lower in energy. It may be seen from Table 8 that for the ring structure the doublet-

quartet energy separation is 0.34 eV for NbC_7 , whereas the two electronic states are nearly degenerate for NbC_6 . The closer energy of the quartet and doublet electronic states may also be seen for other smaller even-numbered carbide clusters, whereas odd numbered carbide clusters exhibit a considerably larger energy splitting, as seen from Figure 2.

Computed Thermodynamic Properties and Vibrational Frequencies. Experimental calculation of thermodynamic functions proceeds through the second or third law methods. These techniques require some knowledge of the structure of the molecule under consideration. Our computed geometries would be quite useful in calculating these properties from experimentally derived data.

The third-law enthalpies for the reaction $\text{Nb}(g) + n\text{C}(\text{graphite}) = \text{NbC}_n(g)$ as a function of temperature are given by

$$\Delta H_0^0 = -RT \ln K_p(T) - T\Delta[(G_T^0 - H_0^0)/T]$$

where $K_p(T)$ is the equilibrium constant, $\Delta[(G_T^0 - H_0^0)/T]$ is the Gibbs energy function (GEF) change for the reaction. The heat content function as a function of temperature is defined as $[(H_T^0 - H_0^0)]$. Consequently, it would be useful to compute the Gibbs free energy functions and enthalpies as a function of temperature so that these results could be used in any potential experimental thermodynamic measurements. Theoretically computed Gibbs free energy functions and heat capacity functions are shown in Table 10.

The theoretically determined heat content functions depend mainly on the quality of the electronic energy calculations. On the basis of our past computations on other transition metal carbides, we believe that both MRSDCI and DFT/B3LYP techniques yield good thermodynamic data. The computed results in Table 10 were derived from the MRSDCI results for the ground and excited states for NbC_n up to $n = 5$ and for larger clusters the DFT data on the ground and excited states were utilized.

As seen from Table 10, an interesting feature is that the GEF and heat capacity functions for NbC_6 at 298 K is unusually larger in magnitude. This is also consistent with its linear ground-state geometry compared to other clusters, which exhibit ring ground-state geometries.

Table 11 reports the computed vibrational frequencies of the normal modes of the smaller clusters and the corresponding infrared intensities. As seen from Table 11, of the six normal modes for NbC_3 , three modes are very intense, two modes are

TABLE 10: Thermodynamic Properties of NbC_n ($n = 3-7$) as a Function of Temperature

	NbC ₃						
<i>T</i> (K)	298.15	2000	2200	2400	2600	2800	3000
GEF (J/molK)	-239.2	-341.8	-348.8	-355.0	-360.8	-366.1	-371.2
Δ <i>H</i> (kJ/mol)	11.6	138.4	154.8	171.3	188.0	204.7	221.6
	NbC ₄						
GEF (J/molK)	-257.4	-391.5	-400.2	-408.3	-415.8	-422.8	-429.4
Δ <i>H</i> (kJ/mol)	14.3	181.1	202.3	223.6	245.0	266.3	287.7
	NbC ₅						
GEF (J/molK)	-270.6	-428.1	-438.6	-448.4	-457.6	-466.2	-474.3
Δ <i>H</i> (kJ/mol)	16.2	219.0	245.6	272.3	299.3	326.5	353.8
	NbC ₆ (DFT excited states)						
GEF (J/molK)	-291.8	-491.6	-504.5	-516.4	-527.5	-537.9	-547.7
Δ <i>H</i> (kJ/mol)	22.3	267.2	299.1	331.0	363.1	395.3	427.6
	NbC ₇ (DFT excited states)						
GEF (J/molK)	-283.2	-491.5	-505.9	-519.3	-531.9	-543.6	-554.7
Δ <i>H</i> (kJ/mol)	20.2	299.8	336.3	373.0	409.7	446.4	483.1

TABLE 11: Frequencies and Their IR Intensities for NbC_n (n = 3–7)^a

		NbC ₃		
freq	470.2	590.1	634.1	
inten	36.4	6.6	28.9	
freq	868.5	1253.4	1522.8	
inten	0.2	4.4	19.9	
		NbC ₄		
freq	291.2	351.1	428.9	
inten	8.9	17.6	39.5	
freq	503.8	571.2	597.7	
inten	0.0	0.3	10.0	
freq	1051.5	1611.6	1815.9	
inten	6.1	9.7	0.9	
		NbC ₅		
freq	93.4	328.0	482.4	
inten	44.0	0.5	17.1	
freq	488.1	500.6	519.5	
inten	15.7	0.2	0.0	
freq	559.5	723.5	1079.5	
inten	60.4	16.0	9.0	
freq	1117.7	1501.8	1744.9	
inten	15.2	13.4	264.9	
		NbC ₆		
freq	49.7	49.8	143.4	
inten	0.6	0.6	21.5	
freq	143.4	264.9	265.0	
inten	21.5	0.1	0.1	
freq	315.3	508.75	508.7	
inten	29.8	3.1	3.1	
freq	578.4	578.4	802.3	
inten	11.1	11.1	35.5	
freq	1326.7	1858.8	2112.5	
inten	48.3	1268.8	27.6	
freq	2213.5			
inten	4368.0			
		NbC ₇		
freq	130.4	219.6	221.1	
inten	4.4	10.6	1.7	
freq	224.3	445.0	477.3	
inten	3.2	8.9	5.4	
freq	508.7	521.1	524.1	
inten	0.0	1.3	18.7	
freq	545.5	591.4	723.6	
inten	20.8	122.5	71.8	
freq	1043.7	1183.2	1420.3	
inten	10.9	7.8	6.0	
freq	1630.5	1908.2	1928.2	
inten	21.0	206.6	768.7	

^a All frequencies are in cm⁻¹ and IR intensities are in KM/mol.

moderately intense, and one mode is weak. The three prominent features of NbC₃ occur at 470, 634, and 1523 cm⁻¹, respectively. There are very intense vibrational modes for other larger clusters, which are potentially observable in the IR spectra.

The Nature of Bonding in NbC_n. The bonding in NbC_n, especially in the region where Nb–C bonds are formed is primarily determined by charge transfer from Nb to C and back transfer from C to Nb. The Nb–C bonds thus exhibit ionic character, as a consequence of electronic charge transfer from Nb to the carbons. Most of the charge transfer goes to the immediate neighbors of Nb. The general trend is that the electron transfer from Nb is larger when it is bound to two or more carbon atoms in contrast to a terminally bound Nb. The ionicity of the Nb–C bonds is directly proportional to the extent of charge transfer. This results in large dipole moments for the electronic states of NbC_n. For example, the ground-state dipole moments of NbC₄ and NbC₅ clusters are 6.3 and 7.7 D, respectively with the dipole vector in the Z direction with Nb⁺C⁻ polarity.

TABLE 12: Leading Configurations for the Electronic States of NbC_n

		NbC ₃	
state	configuration		
² A ₁	(5a ₁) ² (2b ₁) ² (4b ₂) ² (1a ₂) ² (6a ₁) ¹		
⁴ B ₂	(5a ₁) ² (2b ₁) ² (4b ₂) ² (6a ₁) ¹ (3b ₁) ¹ (1a ₂) ¹		
⁶ A ₁	(5a ₁) ² (2b ₁) ² (3b ₂) ² (6a ₁) ¹ (7a ₁) ¹ (3b ₁) ¹ (4b ₂) ¹ (1a ₂) ¹		
		NbC ₄	
state	configuration		
⁴ B ₁	(6a ₁) ² (2b ₁) ² (4b ₂) ² (1a ₂) ² (7a ₁) ¹ (8a ₁) ¹ (3b ₁) ¹		
² A ₁	(7a ₁) ² (2b ₁) ² (4b ₂) ² (1a ₂) ² (8a ₁) ¹		
⁶ A ₁	(6a ₁) ² (2b ₁) ² (3b ₂) ² (1a ₂) ² (7a ₁) ¹ (8a ₁) ¹ (3b ₁) ¹ (4b ₂) ¹ (2a ₂) ¹		
		NbC ₅	
² A ₁	(7a ₁) ² (3b ₁) ² (5b ₂) ² (1a ₂) ² (8a ₁) ¹		
⁴ A ₁	(7a ₁) ² (2b ₁) ² (5b ₂) ² (1a ₂) ² (8a ₁) ¹ (3b ₁) ¹ (4b ₁) ¹		
⁶ A ₂	(6a ₁) ² (2b ₁) ² (5b ₂) ² (1a ₂) ² (7a ₁) ¹ (8a ₁) ¹ (3b ₁) ¹ (4b ₁) ¹ (2a ₂) ¹		
		NbC ₆	
state	configuration		
quo	(9σ) ² (4π) ⁴ (10σ) ¹ (1δ) ²		
dou	(10σ) ² (4π) ⁴ (1δ) ¹		
sext	(8σ) ² (4π) ⁴ (9σ) ¹ (10σ) ¹ (11σ) ¹ (1δ) ²		
		NbC ₇	
state	configuration		
² A ₁	(8a ₁) ² (3b ₁) ² (7b ₂) ² (2a ₂) ² (9a ₁) ¹		
⁴ B ₂	(8a ₁) ² (3b ₁) ² (7b ₂) ² (1a ₂) ² (9a ₁) ¹ (4b ₁) ¹ (2a ₂) ¹		
⁶ A ₁	(8a ₁) ² (3b ₁) ² (6b ₂) ² (1a ₂) ² (9a ₁) ¹ (10a ₁) ¹ (4b ₁) ¹ (7b ₁) ¹ (2a ₂) ¹		
		NbC ₈	
state	configuration		
⁴ B ₁	(9a ₁) ² (3b ₁) ² (7b ₂) ² (2a ₂) ² (10a ₁) ¹ (11a ₁) ¹ (4b ₁) ¹		
² B ₁	(10a ₁) ² (4b ₁) ² (5b ₂) ² (2a ₂) ² (5b ₁) ¹		
⁶ A ₁	(9a ₁) ² (3b ₁) ² (5b ₂) ² (2a ₂) ² (10a ₁) ¹ (11a ₁) ¹ (12a ₁) ¹ (4b ₁) ¹ (5b ₁) ¹		

The Mulliken populations of the clusters are consistent with the charge transfer from Nb to C. For example, the gross Mulliken populations of Nb in NbC₄ and NbC₅ are 4.11 and 3.92, respectively. These values deviate from the natural Nb population of 5.0 suggesting strong electron transfer from Nb to C. It can be seen that the charge transfer from Nb is mainly from its 5s orbital to the C(2p) orbital. It is quite interesting that the 4d orbital of Nb does not participate in the charge-transfer process. The electron densities of the 4d and 5p orbitals of Nb are enhanced due to rearrangement of orbitals upon bond formation and back transfer of electronic charge from C to Nb(4d) and Nb(5p) due to pπ–pπ and dπ–pπ back-bonding. For example, the carbon atoms in NbC₄ exhibit gross populations of 4.23 and 4.21. Likewise, the carbon atoms in NbC₅ exhibit gross populations of 4.3, 4.28, and 3.93. The single carbon atom farthest away from Nb in the NbC₅ ring structure has the smallest population. It is interesting that charge transfer from Nb to the nearest carbons attached to it is delocalized at least to the second neighbors. It is also quite interesting that the Nb(5p) populations are between 0.14 and 0.3. For example, the Nb(5p) populations in NbC₄ and NbC₅ are 0.19 and 0.14, respectively in their ground states. Thus, the Nb atom deviates from its atomic population not only due to charge transfer from Nb to carbons but also due to rearrangement of the atomic populations among the 5s, 5p, and 4d orbitals due to back transfer from C to Nb and hybridization.

Table 12 shows the leading configurations of the electronic states of NbC_n. As seen from Table 12, the ²A₁ ground state of NbC₃ with the ring structure has a leading configuration with a single electron in the 6a₁ orbital, all other lower energy orbitals being doubly occupied. The ⁴B₂ state arises from the promotion of an electron from the 1a₂ orbital to the 3b₁ orbital relative to the ground state. On the other hand, ⁶A₁ state arises from another excitation of 4b₂ into 7a₁ in addition to the 1a₂ to 3b₁ excitation.

The highest occupied and lowest unoccupied MOs of NbC₃ can be described as follows. The 1a₂ orbital can be described as

$$1a_2 = \text{Nb}(4d_{xy}) + C_2(2p_x) - C_3(2p_x)$$

where C₂ and C₃ atoms are equivalent. The 4b₂ orbital can be expressed as

$$4b_2 = \text{Nb}(4d_{yz}) + C_2(2s) - C_3(2s) + C_2(2p_y) + C_3(2p_y)$$

whereas the 6a₁ orbital is composed of

$$6a_1 = \text{Nb}(4d_{z^2-(x^2+y^2)}) + \text{Nb}(5s)$$

The lowest unoccupied 3b₁ molecular orbital (LUMO) is composed of

$$3b_1 = \text{Nb}(4d_{xz}) + C_1(2p_x)$$

The singly occupied 6a₁ orbital is thus predominantly on Nb. The above compositions of the occupied orbitals are consistent with the description of bonding and Mulliken populations.

We expect the spin-orbit splittings of NbC_n to be rather small on the basis of our previous estimate for NbC₂ from the atomic Nb splitting. The Nb ⁶D(4d⁴5s¹) ground-state splits into *J* = 1/2, 3/2, 5/2, 7/2, and 9/2 atomic states by 1050 cm⁻¹ between the highest and lowest *J* states. On the other hand, the ⁴F(4d³5s²) spin-orbit splitting is 1663 cm⁻¹. Because the Nb Mulliken populations of the ground state of NbC₂ are closer to the 4d⁴5s¹ configuration rather than 4d³5s² due to the charge transfer from Nb to C, the ground-state spin-orbit splitting between the two E_{1/2} states of NbC₂ was estimated to be about 400 cm⁻¹. Therefore, we do not expect the spin-orbit splitting to be large for NbC_n clusters.

V. Conclusion

We have reported the results of the CASMCSF/MRSDCI computations of NbC_n for *n* = 3–5 and DFT/B3LYP computations for the doublet, quartet, and sextet electronic states of NbC_n for *n* = 3–8. We have considered five different geometries, viz., ring (R), linear (L), kite (K), Nb-terminally bound to a C_n ring (T), and a structure with C–Nb–C bridge fused with a C_n ring (A). We find that the NbC_n clusters exhibit an odd–even alternation pattern in that for even *n*, the linear and ring structures are close in energy, while the odd-*n* clusters exhibit substantially lower ring structures. Among the clusters considered here, NbC₆ was found to be very special in having a linear geometry as the ground state. We have computed the equilibrium geometries, energy separations of the low-lying electronic states, Gibbs free energies, and the heat capacity functions as a function of temperature. The DFT/B3LYP technique was found to yield geometries and energy separations in overall agreement with the CASMCSF/MRSDCI techniques. The nature of bonding in these carbide clusters was found to be very ionic with Nb⁺C⁻ bonding facilitated by charge transfer from Nb(5s) to C(2p). This was accompanied by back transfer from C(2p) to Nb(4d) and Nb(5p) through ππ–ππ and ππ–δπ bonding.

Acknowledgment. This research was supported by the US Department of Energy under Grant No. DEFG02-86ER13558.

References and Notes

- Heath, J. R.; O'Brien, S. C.; Zhang Q.; Liu, Y.; Curl R. F.; Kroto, H. W.; Tittel, F. K.; Smalley R. E. *J. Am. Chem. Soc.* **1985**, *107*, 7779.
- Clemmer, D. E.; Shelimov, K. B.; Jarrold, M. F. *J. Am. Chem. Soc.* **1994**, *116*, 5971.
- Cassady, C. J.; McElvany, S. W. *J. Am. Chem. Soc.* **1990**, *112*, 4788.
- Gingerich, K. A. *J. Less-Common Metals* **1985**, *110*, 41. Gingerich, K. A. *Curr. Top. Mater. Sci.* **1980**, *6*, 345. Gingerich, K. A.; I. Shim, I. In *Advances in Mass Spectroscopy 1985*; Todd, J. F. J., Ed.; Wiley: New York, 1986; p 1051.
- Rohmer, M.; Benard, M.; Poblet, J.-M. *Chemical Reviews* **2000**, *100*, 495.
- Pelino, M.; Haque, R.; Bencivenni, L.; Gingerich, K. A. *J. Chem. Phys.* **1988**, *88*, 6534.
- Pelino, M.; Gingerich, K. A.; Haque, R.; Bencivenni, L. *J. Phys. Chem.* **1986**, *90*, 4358.
- Shim, I.; Pelino, M.; Gingerich, K. A.; *J. Chem. Phys.* **1992**, *97*, 9240.
- Shelimov, K. B.; Clemmer, D. E.; Jarrold, M. F. *J. Phys. Chem.* **1995**, *99*, 11 376.
- Clemmer, D. E.; Shelimov, K. B.; Jarrold, M. F. *Nature* **1994**, *367*, 718.
- Shelimov, K. B.; Clemmer, D. E.; Jarrold, M. F. *J. Phys. Chem.* **1994**, *98*, 12 819.
- Simard, B.; Presunka, P. I.; Loock, H. P.; Berces, A.; Launila, O.; *J. Chem. Phys.* **1997**, *107*, 307.
- Simard, B.; Hackett, P. A.; Balfour, W. J. *J. Chem. Phys.* **1997**, *107*, 307.
- Hamrick, Y. M.; Weltner, W., Jr. *J. Chem. Phys.* **1991**, *94*, 3371.
- Van Zee, R. J.; Bianchini, J. J.; Weltner, W., Jr. *Chem. Phys. Lett.* **1986**, *127*, 314.
- Brom, J. M.; Graham, W. R. M.; Weltner, W., Jr. *J. Chem. Phys.* **1972**, *57*, 4116.
- Weltner, W., Jr. *Magnetic Atoms and Molecules*; Dover Publications: New York, 1983.
- Li, X.; Liu, S. S.; Chen, W.; Wang, L. S. *J. Chem. Phys.* **1999**, *111*, 2464.
- Langenberg, J. D.; Shao, L.; Morse, M. D. *J. Chem. Phys.* **1999**, *111*, 4077.
- Langenberg, J. D.; DaBell, R. S.; Shao, L.; Dreesen, D.; Morse, M. D. *J. Chem. Phys.* **1998**, *109*, 7863.
- Simard, B.; Hackett, P. A.; Balfour, W. J. *Chem. Phys. Lett.* **1994**, *230*, 103.
- Barnes, M.; Merer, A. J.; Metha, G. F. *J. Chem. Phys.* **1995**, *103*, 8360.
- Rozsak, S.; Balasubramanian, K. *J. Chem. Phys.* **1997**, *106*, 158.
- Rozsak, S.; Balasubramanian, K. *J. Phys. Chem.* **1997**, *101*, 2666.
- Rozsak, S.; Balasubramanian, K. *Chem. Phys. Lett.* **1997**, *264*, 80.
- Rozsak, S.; Balasubramanian, K. *Chem. Phys. Lett.* **1997**, *265*, 553.
- Majumdar, D.; Balasubramanian, K. *Chem. Phys. Lett.* **1997**, *280*, 212.
- Tan, H.; Liao, M. Z.; Balasubramanian, K. *Chem. Phys. Lett.* **1997**, *280*, 219.
- Tan, H.; Liao, M. Z.; Balasubramanian, K. *Chem. Phys. Lett.* **1997**, *280*, 423.
- Majumdar, D.; Balasubramanian, K. *Chem. Phys. Lett.* **1998**, *284*, 273.
- Dai, D. G.; Balasubramanian, K. *J. Phys. Chem. A*, in press.
- Shim, I.; Gingerich, K. A. *J. Chem. Phys.* **1982**, *76*, 3833.
- Shim, I.; Gingerich, K. A. *Surface Science* **1985**, *156*, 623.
- Shim, I.; Finkbeiner, H. C.; Gingerich, K. A. *J. Phys. Chem.* **1987**, *91*, 3171.
- Shim, I.; Gingerich, K. A. *J. Chem. Phys.* **1997**, *106*, 8093.
- Pacchioni, G.; Koutecky, J.; Fantucci, P. *Chem. Phys. Lett.* **1982**, *92*, 486.
- Russo, N.; Andzelm, J.; Salahub, D. R. *Chemical Physics*, **1987**, *114*, 331.
- Tan, H.; Dai, D.; Balasubramanian, K. *Chem. Phys. Lett.* **1998**, *286*, 375.
- Cartier, S. F.; May, M. B.; Castleman, A. W., Jr. *J. Am. Chem. Soc.* **1994**, *116*, 5295.
- McElvany, S. W.; Cassady, C. J. *J. Phys. Chem.* **1990**, *94*, 2057.
- Wei, S.; Guo, B. C.; Deng, H. T.; Kerns, K.; Purnell, J.; Buzza, S.; Castleman, A. W., Jr. *J. Am. Chem. Soc.* **1994**, *116*, 4475.
- Pilgrim, J. S.; Brock, L. R.; Duncan, M. A. *J. Phys. Chem. A* **1995**, *99*, 544.
- Yeh, C. S.; Byun, Y. G.; Afzaal, S.; Kan, S. Z.; Lee, S.; Freiser, B. S.; Hay, P. J. *J. Am. Chem. Soc.* **1995**, *117*, 4042.
- Fan, W. J.; Wang, L.-S. *J. Phys. Chem.* **1994**, *98*, 11 814.
- Arbuznikov, A. V.; Hendrickx, M.; Vanquickenborne, L. G. *Chem. Phys. Lett.* **1999**, *310*, 515.
- Nash, B. K.; Rao, B. K.; Jena, P. *J. Chem. Phys.* **1996**, *105*, 11 020.
- Balasubramanian, K. *Relativistic Effects in Chemistry. Part A: Theory and Techniques*; Wiley-Interscience: New York, 1997; p 301. Balasubramanian, K. *Relativistic Effects in Chemistry. Part B: Applications*; Wiley-Interscience: New York, 1997; p 531.

- (48) La John, L. A.; Christiansen, P. A.; Ross, R. B.; Atashroo, T.; Ermler, W. C. *J. Chem. Phys.* **1987**, *87*, 2812.
- (49) Balasubramanian, K. *J. Chem. Phys.* **1988**, *89*, 5731.
- (50) Pitzer, R. M.; Winter, N. W. *J. Phys. Chem.* **1988**, *92*, 3061.
- (51) The major authors of ALCHEMY II are Lengsfeld, B.; Liu, B.; Yoshmine, Y.
- (52) Balasubramanian, K. *Chem. Phys. Lett.* **1986**, *127*, 585.
- (53) Tan, H.; Liao, M. Z.; Balasubramanian, K. *J. Phys. Chem. A* **1998**, *102*, 6801.
- (54) Pyykkö, P.; Tamm, T. J. *J. Phys. Chem. A* **1997**, *101*, 8107.
- (55) Becke, A. D. *J. Chem. Phys.* **1993**, *98*, 5648.
- (56) Gaussian 98, Revision A.7, Frisch, M. J.; Trucks, G. W.; Schlegel, H. B.; Scuseria, G. E.; Robb, M. A.; Cheeseman, J. R.; Zakrzewski, V. G.; Montgomery, J. A., Jr.; Stratmann, R. E.; Burant, J. C.; Dapprich, S.; Millam, J. M.; Daniels, A. D.; Kudin, K. N.; Strain, M. C.; Farkas, O.; Tomasi, J.; Barone, V.; Cossi, M.; Cammi, R.; Mennucci, B.; Pomelli, C.; Adamo, C.; Clifford, S.; Ochterski, J.; Petersson, G. A.; Ayala, P. Y.; Cui, Q.; Morokuma, K.; Malick, D. K.; Rabuck, A. D.; Raghavachari, K.; Foresman, J. B.; Cioslowski, J.; Ortiz, J. V.; Baboul, A. G.; Stefanov, B. B.; Liu, G.; Liashenko, A.; Piskorz, P.; Komaromi, I.; Gomperts, R.; Martin, R. L.; Fox, D. J.; Keith, T.; Al-Laham, M. A.; Peng, C. Y.; Nanayakkara, A.; Gonzalez, C.; Challacombe, M.; Gill, P. M. W.; Johnson, B.; Chen, W.; Wong, M. W.; Andres, J. L.; Gonzalez, C.; Head-Gordon, M.; Replogle, E. S.; Pople, J. A. Gaussian, Inc., Pittsburgh, PA, 1998.
- (57) Moore, C. E. *Tables of Atomic Energy Levels, Vol II*; US National Institute of Standards and Technology: Washington, D. C. 1979.